1972

# Failure tests of rectangular modal box girders, April 1972 73-38 & 74-13

J. A. Corrado

B. T. Yen

# FAILURE TESTS OF RECTANGULAR MODEL BOX GIRDERS

(DRAFT)

by

Joseph A. Corrado

Ben T. Yen

April 1972

Fritz Engineering Laboratory Report No. 380.2

# FAILURE TESTS OF RECTANGULAR MODEL BOX GIRDERS[a]

By Joseph A. Corrado[1], A.M., ASCE and Ben T. Yen[2], M. ASCE

## INTRODUCTION

The use of thin-walled steel box girders as the main load-carrying members in bridge structures has recently gained considerable popularity in this country. This can be attributed to an increased awareness of the structural efficiency, financial savings and pleasing aesthetic appearance which can be achieved with such a configuration (1).

To date, most research on steel box girders has been concerned with the behavior of the member in the linear, prebuckling range. Little attention has been focused on the evaluation of the modes of failure and load-carrying capacity of such members.

In hope of advancing the state-of-the-art for the design of box girders and in light of research needs suggested by the ASCE-AASHO Subcommittee on Box Girders (2), a combined experimental and analytical study was initiated and had as its main goals the following: (1) an evaluation, through use of model tests, of the post-buckling behavior, modes of failure and load-carrying capacity of single-span, rectangular steel box girders and (2) the development of a preliminary analytical method for estimating the load-carrying capacity of such box girders. Only the experimental phase of this study is reported here.

---

[a]Presented at the October 18-22, 1971, ASCE Annual Meeting and National Meeting on Environmental Engineering, St. Louis, Missouri

[1]Structural Engineer, Department of Structural Mechanics, Naval Ship R & D Center, Bethesda, Maryland, formerly Instructor, Civil Engineering Department, Lehigh University, Bethlehem, Pennsylvania

[2]Associate Professor, Civil Engineering Department, Lehigh University, Bethlehem, Pennsylvania

## DESCRIPTION OF TEST SPECIMENS

Two rectangular model box girders having a vertical axis of symmetry were fabricated from sheet steel and are shown in Fig. 1. The prime consideration in the design of the specimens was based on the procurement of a qualitative evaluation of the post-buckling behavior and failure mechanisms for single-span box girders subjected to shear, bending and torsion. Initiation of failure in the web plates was of particular interest and governed, to a large degree, the design of the relative dimensions of the specimen component parts.

Each of the two specimens were formed by connecting two flat flange plates to two webs which had previously been bent into channel shapes. The flanges of the web channels facilitated the longitudinal connections.

Careful consideration was given to a possible connection medium. It was felt that tensile forces which had to be carried by the joints during the post-buckling range of loading would be most critical. Therefore a series of tensile tests were performed using several different joints. A 50-50 solder (50% Tin, 50% Lead) produced satisfactory joints with only small amounts of web distortions and was selected. During the soldering process, the component flange and web plates were securely positioned by mechanical fasteners which passed through predrilled holes. These fasteners were left in place after fabrication and during testing.

The first test specimen, designated M1 (Fig. 1) consisted of a box section 3 inches deep by 4 inches wide and had a span length of 24 inches. The nominal slenderness ratio (depth.thickness) for the webs was 192. This conformed to the limiting value given in the current AASHO specifications (3) for the web plates of plate girders. Transverse stiffeners attached to

the exterior surface divided the webs into panels having aspect ratios (length/depth) ranging from 1.0 to 1.67. Solder, the same as that used for the longitudinal web-to-flange joints, was used to attach all transverse stiffeners. The top flange having a width of 7 inches and 5/64-inch thickness had been sized to simulate the deck of a composite box girder bridge. Cross-bracing (X) was provided at the loading and support points for the purpose of distributing the concentrated loads and maintaining the shape of the cross section for the entire range of loading. Intermediate bracing was provided at one additional location.

Specimen M2 (Fig. 1) had a configuration very similar to that of M1. The major differences were in the width of the top flange and the elimination of both the transverse stiffeners on the bottom flange and the intermediate X-bracing.

The component plate dimensions and material properties are listed in Table 1. Material properties were obtained from standard tensile specimens (ASTM E8) which had been cut from the original steel sheets in the direction parallel to the longitudinal axis of the specimens.

## INSTRUMENTATION AND TEST SETUP

Instrumentation for both specimens consisted of dail gages and electrical-resistance strain gages. Dial gages were utilized to monitor the vertical and rotational displacement of each specimen. Rectangular strain gage rosettes were mounted in back-to-back pairs at the center of several web panels on both sides of the cross section. Back-to-back gages were used so that stresses by in-plane bending and shear could be isolated from the out-of-plane bending stresses. Several linear gages on specimen

M1 were used to check the normal stress distribution over the cross section. A coat of whitewash was applied to M2 for visual signs of yielding. Whitewash was not utilized on M1.

For identification purposes each panel of the box girders was assigned a number as indicated in Fig. 1. A panel is a longitudinal segment of the member between transverse web stiffeners. The two webs of a box girder were designated as "north" and "south". Thus, the designation 1S and 1N refer to the south and north webs of panel 1, respectively.

The specimens were tested as simply supported members in a 120,000 pound capacity, Tinius Olsen screw type testing machine. Load was applied mechanically through a spreader bar to the specimen (Fig. 2). By carefully varying the longitudinal and transverse position of the specimen with respect to the movable head of the machine, desired combinations of bending and torsion were produced. The loading configuration and corresponding shear, bending moment and twisting moment diagrams for specimens M1 and M2 are respectively indicated in Figs. 3 and 4.

## TESTING OF SPECIMENS

In the following discussions it is defined that an unsymmetrical load subjected the member to torsion in addition to bending, whereas symmetrical loads produced only bending.

For all tests the strain rate in terms of free travel of the testing machine's movable crosshead was approximately 0.025 inches per minute. The actual travel speed under load was somewhat less than this. Data readings were initiated almost immediately after a given load level had been attained. Some drop in load occurred during the 20 to 30 minute intervals

of data readings while the vertical deflections remained perfectly stable. In the linear-elastic range of girder behavior these load drops were small (20-40 pounds). However, they were as large as 250 pounds in the inelastic range. Such phenomenon was unexpected, especially in the linear-elastic range. Because of the qualitative nature of the study, it was not given serious consideration during testing of the specimens.

SPECIMEN M1 (Unsymmetrical Loading) - Prior to the failure test under unsymmetrical loading, two identical series of symmetrical loads were applied to check out the overall behavior of the member and the repeatability of the test data. A comparison of the test data from the two series of loads indicated that repeatability was achieved.

The unsymmetrical loading condition can be seen in Fig. 3. With the load at midspan and directly over the north web, each half-span was subjected to identical bending, shear and torsion. Load was applied and data recorded at each 200 pound increment up to 1375 pounds when buckling of the web and transverse stiffener occurred directly under the load point. The specimen was unloaded and repairs effected by straightening and strengthening the loading stiffener. Testing was resumed and at 1200 pounds considerable additional local buckling of the web was noticed at the same location although no evidence of stiffener buckling could be seen. Further inspection uncovered tearing of the upper portion of the solder joint connecting the loading stiffener to the web. Prior to this, bulging of the web along the tension diagonals of web panels 1N, 2N, 4N and 6N was clearly observed.

Repairs this time included straightening of the buckled web on the north side and the attachment of a heavy angle stiffener to each web at the load

point location. The eccentricity of load was shifted to the south side and load was cycled several times between 0 and 1000 pounds again to check repeatability.

Final testing proceeded without incident up to 1200 pounds. Full sets of deflection and strain measurements were recorded for each 200 pound increment. At 1400 pounds the first definite signs of tension diagonal web bulging appeared in panel 6S. Loading continued and at 1500 pounds tension field action was very prominent in web panels 1S and 6S which had aspect reatios of 1.67 and 1.5, respectively. No visual evidence of tension field action could be detected in the corresponding web panels on the north side. It is significant to point out again that the load for this test was directly above the web on the south side. Upon further loading to 1600 pounds, a sharp cracking noise was heard and a portion of the top flange near the centerline of the specimen started to distort downwards on the south side. Large distortions of the cross section were beginning to take place. Later inspection indicated that failure of the midspan X-bracing was the cause of the cracking noise. The load was not steady at this point yet additional load could be supported. Pulling up of the bottom flange and pulling down of the top flange at the tension diagonal corners of web panels 1S and 6S started to occur at 1650 pounds. At 1750 pounds web bulging had occurred along the tension diagonals of 2S and 4S in addition to failure of the X-bracing at the east end. A maximum load of 1800 pounds was attained before excessive deflections and cross-sectional deformation prohibited further loading. Even at the maximum load no signs of web bulging could be detected on the north side. Figure 5 clearly shows the permanent deformations. Bulging of the web along the tension diagonals is obvious on the south side but not on the north side.

SPECIMEN M2 (Unsymmetrical Loading) - Symmetrical load applications were made to check the specimen and test setup. Following these, testing under the loading condition indicated in Fig. 4(a) was initiated. The load had an eccentricity of 1-inch to the north side of the cross section. Load was applied in 200 pound increments up to 800 pounds and thereafter in 100 pound increments. Dial gage readings and strain measurements were recorded for each load increment. The first significant observations involved bulging of the web along the tension diagonal of web panels 1N and 2N at about 1200 pounds. Further loading produced additional bulging and at 1700 pounds flaking of the whitewash along the tension diagonal of web panel 2N had occurred. Similar but less severe web deformations were observed in web panels 1S and 2S. None of the other web panels exhibited any signs of such deformations at this load level. After a short pause in testing during which time the load had been decreased to 400 pounds, loading was resumed using 100 pound increments. A load of 1800 pounds produced pulling up of the bottom flange at the lower tension field corner of web panel 2N. Web bulging also had begun in web panel 5N. Visual inspection revealed the absence of any noticeable cross-sectional deformations. Loading continued and caused additional bulging in web panel 2N while no further increases in web deformations of 1N could be detected. At 1900 pounds, web panel 2S exhibited considerable bulging along the tension diagonal. Shortly thereafter, the maximum load of 1930 pounds was attained. Unloading followed and the resulting permanent web deformations are shown in Fig. 6.

SPECIMEN M2 (Symmetrical Loading) - After failure of panel 2 under unsymmetrical loading the remaining portion of specimen M2 was further

tested under symmetrical loading. Figure 7 shows the setup. It also depicts the absence of damage or permanent deformations in panels 3, 4, 5 and 6 during the earlier unsymmetrical load test. For the shortened span the symmetrical load subjected the specimen to high flexural shear, a moderate amount of bending moment and no torsion (Fig. 4(b)). Failure was expected to occur in either panel 4 or 5.

The testing procedure was very similar to that employed in the previous tests. The first visual signs of tension field action showed up in both webs of panel 5 at 1700 pounds. The lateral deformations of the webs in this panel increased as loading continued but were not excessive even at 2400 pounds. The next increment of load produced the first noticeable signs of web bulging in web panels 4S and 4N, simultaneously. At 2530 pounds, flaking of the whitewash occurred along the tension diagonals of web panels 4S, 4N, 5S and 5N. Additional loading caused the web deformation on both sides of panels 4 and 5 to grow excessively. This was accompanied by vertical deformations of the flanges over the length of these panels. The maximum load that could be reached was 2650 pounds. Final deformation patterns are indicated in Fig. 8.

## DISCUSSION OF TEST RESULTS

RESULTS OF SYMMETRICAL LOAD TEST - Symmetrical loading would theoretically produce identical shear and normal stresses in the two webs of a specimen. For specimen M2, with the larger of the two shear span-to-depth ratios being about 2.6 and the neutral axis positioned approximately 1/4 the web depth from the compression flange, shear was anticipated to govern the mode of failure. A plot of the vertical shear stresses at the centerline of web panel 5 (Fig. 9) indicates the close equivalence of stresses

for the webs for the entire range of loading. The stresses in this figure have been obtained by averaging the measured surface strains and are assumed to be uniform through the thickness of the plates. This is also the case for all other stress plots.

Tension field action was anticipated and observed in web panels 4 and 5. Figure 10 illustrates the direction and magnitude of the principal stresses for panel 5 at three distinct load levels. The angle between the maximum principal stress and a horizontal axis is theoretically $45^{o}$ for pure shear during the early stages of loading when the shear is carried through simple beam action. As the load increases and the shear exceeds the theoretical web buckling load, the principal stresses are gradually reoriented in the direction of the tension diagonal of the panel. Such a phenomenon was common in the other tests reported herein, and is typical of web plates of plate girders subjected to shear and combined bending and shear (4). The symmetricity of loading and stress magnitudes in the two webs of a panel is also demonstrated by this figure.

The overall behavior of the specimen can best be described by referring to the load-deflection curve in Fig. 11. The response was essentially linear up to 2500 pounds. In the previous section it was noted that excessive web bulging and flaking of the whitewash occurred along the tension diagonals of web panels 4S and 4N at 2530 pounds. Strain readings indicated that yielding initiated in both webs of panel 5 at 2550 pounds. With the webs yielding and able to carry little or no additional shear, the load-deflection curve became almost flat. A small amount of additional load was realized through the transverse shear strength of the flanges after the webs had failed. Evidence of this was obtained through the recording of large

increase in the top flange bending strains of panel 4 at 2500 pounds. This can be compared with the frame action contribution of plate girder flanges described by Chern and Ostapenko (5). As depicted in Fig. 11, the maximum load of 2650 pounds was more than twice as large as the theoretical buckling loads for panels 4 and 5, which were computed assuming the web boundaries to be fixed along the flanges and simply-supported along the transverse stiffeners.

The data points marked with x's in the inelastic region of the load-deflection plot of Fig. 11 were recorded at the end of each data acquisition time period. These lower load levels were a result of the load drops previously described. A brief supplementary study, performed after testing had been completed, revealed that this type of behavior was due to a combination of the non-zero strain rate used during loading and relaxation of the solder joints. The limited scope of this supplementary study did not permit precise separation of the effects of strain rate and joint relaxation. However, it was evident that the effects of the non-zero strain rate were dissipated during the 20 to 30 minute period used for taking data readings and during which the deflection of the member was stable. This is analogous to the behavior associated with tensile coupon tests, in which the dynamic yield load decreases to the static yield load within a period of about five minutes (6). Because of the inability to accurately separate the effects of joint relaxation and strain rate, it can only be reasoned that the statically applied loads, that is, those loads corresponding to a zero strain rate, lie between the upper (o) and lower (x) data points.

In conclusion, it is clear that the mode of failure of symmetrically loaded box girders is yielding along the web tension diagonals accompanied

by deformation of the flanges, providing premature failure of the compression flange is prevented. The behavior and failure mode compare quite well with that of similarly loaded plate girders.

RESULTS OF UNSYMMETRICAL LOAD TESTS - Under this loading configuration two tests were performed, one each on specimens M1 and M2. The results of specimen M2 are discussed first.

Figure 4(a) indicates the combination of shear, bending and torsion applied to this specimen. Due to the loading condition and geometry of the specimen, a shear type failure was again expected. Therefore, the vertical shear stress at the midpoint of the web would be an appropriate indicator of the behavior of the specimen. A theoretical evaluation of the shearing stresses resulting from flexure and St. Venant torsion indicated that these stresses would be largest in web panels 1N and 2N. Evidence that this actually occurred during testing can be seen in Fig. 12. Correlation with the theoretical values described above is also evident.

A complete evaluation and understanding of the behavior of the specimen up to ultimate load requires a correlated review of the load-deformation and load-stress data. The load-deflection curve in Fig. 13 shows that the overall response was linear up to 1500 pounds. Thereafter, the slope of the curve gradually decreases, indicating a gradual reduction of girder stiffness. At 1700 pounds, general yielding was observed along the tension diagonal of web panel 2N. Figure 12 verifies this and also indicates that the shear stress begins to decrease in web panel 1N and increase in web panels 1S and 2S upon the application of additional load. This implies that a redistribution of the shear has taken place. Web panel 2N, which has experienced general yielding, could not carry any more shear

and therefore any additional flexural shear was carried by the web on the south side. Yielding of web panel 2N also affected the torsional stiffness of the member as can be seen in Fig. 14. The segment of the member containing panel 2 (the length to the left of the load point) could no longer support its full share of the twisting moment due to its decreased torsional stiffness. Therefore, a greater portion of the twisting moment had to be carried by the section to the right of the loading point. This redistribution phenomenon caused the shear stresses to change. This is clearly indicated in the shear stress plots for panel 5 in Fig. 15.

The change in the load versus shear stress curves of Figs. 12 and 15 can be explained by again simply considering the superposition of the shear flow due to bending and St. Venant torsion. For the given direction of torsion, shear flows add on the north side and subtract on the south side. It is important to note that effects due to warping torsion and distortion of the cross section have been examined. However, because of the rather good correlation between the experimental stresses and those predicted by considering only bending and St. Venant torsion, detailed consideration of warping and distortion is not deemed necessary for evaluation of the behavior of the specimen and the mode of failure [7].

Additional loading eventually caused general yielding along the tension diagonal of web panel 2S (Fig. 12) and an increased rate of deflection (Fig. 13). Prior to the attainment of the maximum load, flange deformations resembling the frame action described in the previous section occurred quite substantially on the north side of panel 2, and to a somewhat lesser degree on the south side of the same panel.

Analogous to the results for symmetrical testing of M2, the data points denoted by circles and x's in the inelastic region of the load-deflection plot of Fig. 13, respectively, represent the upper and lower bounds of the static loads of the unsymmetrical load test of specimen M2.

It is interesting to note that the load-rotation curve in Fig. 14 has not flattened out upon attainment of the maximum load. This infers that the torsional capacity of the member has not yet been exhausted and additional torsional moment could be supported by the undamaged portion to the right of the loading point.

A recapitulation of the pertinent events leading up to the ultimate load will help to define clearly the mode of failure for specimen M2. Initial signs of failure showed up as tension diagonal yielding in the most critical web panel (2N), which has the most severe combination of stresses and geometry. Additional loading produced redistribution of the flexural shear to the other side of the cross section, that is, to web panel 2S. This obviously was accompanied by a redistribution of the normal bending stresses. The decreased torsional stiffness of the shear span containing panel 2N forced a redistribution of the twisting moment to the undamaged right shear span. The maximum load was reached when no additional flexural shear could be supported in panel 2. This took place after panel 2S had exhibited yielding along its tension diagonal and the flanges had been partially deformed due to frame action. Figure 6 portrays the failure mode configuration.

Keeping in mind the behavior and results of M2, attention is next focused on the results of specimen M1. In the final test of M1, the load was at midspan with an eccentricity to the south side. Under such loading

conditions web panels on the south side were subjected to larger shear stresses than those on the north side, and therefore web failure would be expected to initiate on the south side of the cross section. This actually occurred. The lower part of Fig. 16 clearly points out the difference in magnitude of the shear stresses on the north and south sides. The upper part of this figure shows that the relative magnitude of these stresses is reversed when the eccentricity is reversed. The distribution of shear stresses prior to any web failure is quite similar to that obtained for specimen M2 (Fig. 12).

When web failures initiated on the south side, a redistribution of the flexural shear to the north side was expected to occur. Referring again to the lower part of Fig. 16 it is seen that this was not the case. As web panel 4S began to fail through yielding along the tension diagonal, the shear stress in the corresponding web on the north side remained relatively constant. Behavior of this type was also exhibited in panels 1 and 6. This is unlike the behavior of specimen M2 which demonstrated significant redistribution capability (Fig. 12).

The load-deflection and load-rotation curves of Figs. 17 and 18, respectively indicate that little flexural or torsional stiffness remained once web panels 1S and 6S had yielded. This is also quite different than the behavior of M2 which possessed appreciable torsional and flexural stiffness after web panel 2N had yielded. Of course, the lack of torsional stiffness in M1 could be expected because web panel failures occurred almost simultaneously (1S and 6S) in each shear span. (For M2, web failure occurred in only one of the shear spans.) On the contrary, the absence of significant flexural stiffness was not anticipated and must be

attributed to the poor redistribution characteristics of the member. Failure of the midspan X-bracing at approximately 1500 pounds and the resulting cross-sectional deformation certainly had a major adverse effect on the ability to transfer the load from the south web to the north web. Subsequent failure of the X-bracing at the east end compounded the effect.

Thus, specimen M1 failed prematurely due to combined web panel yielding and excessive distortion of the cross section. It is clear that adequate diaphragms or X-bracing must be provided if the member is to provide full redistribution of the flexural shear and torsion and thus develop its true load-carrying capacity.

## CONCLUSIONS

From the results of the tests on two single span, slender-web rectangular model box girders, the following conclusions were reached.

1. The load-carrying capacity of the slender web box girders was not limited to the theoretical web buckling load.

2. A single-span rectangular box girder subjected to high shear and a moderate amount of bending but not torsion (M2) exhibited yielding simultaneously along the tension diagonal of both webs of a box girder panel, resembling the behavior of a web plate in a similarly loaded plate girder. Failure of the box girder occurred when large vertical deformation of the flanges followed extensive tension field yielding, again similar to the failure mechanism of a plate girder.

3. The box girder panels which incurred tension field action and subsequent flange deformation were the box panels having the most severe loading and geometric conditions (panel 4 and 5, M2).

4. When box girders were subjected to shear, bending and torsion, web failure by tension field occurred first in those web plates having the most severe combination of loading and geometry (1S and 6S of M1 and 2N of M2).

5. When one of the two webs of a box girder panel failed, redistribution of shear within the box panel took place provided that it was properly braced to prevent distortion of the girder cross section (panel 2 of M2).

6. The torsional stiffness of a box girder panel was greatly reduced when the box panel experienced web failure due to yielding along the tension diagonal (panel 2 of M2).

7. A box girder panel failed when both its webs developed tension diagonal yielding and followed by deformation of the flanges (panel 2, M2).

8. The shear or bending capacity of a single-span box girder was reached when one of its box panels failed (M2).

9. Torsional stresses had an important effect on the behavior and load-carrying capacity of the model specimen.

10. Premature failure of diaphragms or X-bracing adversely affect the load-carrying capacity of box girders subjected to torsional loads.

## ACKNOWLEDGMENTS

The work summarized herein was performed at Fritz Engineering Laboratory, Department of Civil Engineering, Lehigh University, Bethlehem, Pennsylvania. It is a part of a study on the strength and behavior of box girders. The cooperation of the authors' colleagues is sincerely appreciated.

## APPENDIX 1 - REFERENCES


1. ASCE-AASHO Committee on Flexural Members, "Trends in the Design of Steel Box Girder Bridges," Progress Report, Subcommittee on Box Girder Bridges, Journal of the Structural Division, ASCE, Vol. 93, No. ST3, June 1967.

2. ASCE-AASHO Committee on Flexural Members, "Progress Report on Steel Box Girders," Subcommittee on Box Girders, Journal of the Structural Division, ASCE, Vol. 97, No. ST4, April 1971.

3. Interim Specifications, 1971, American Association of State Highway Officals.

4. Basler, K., Yen, B. T., Mueller, J. A. and Thürlimann, B., "Web Buckling Tests on Welded Plate Girders," WRC Bulletin No. 64, September 1960.

5. Chern, C. and Ostapenko, A., "Ultimate Strength of Plate Girders Under Shear," Fritz Engineering Laboratory Report No. 328.7, Lehigh University, August 1969.

6. Desai, S., "Tension Testing Procedure," Fritz Engineering Laboratory Report No. 237.44-Draft, Lehigh University, February 1969.

7. Wright, R. N., Abdel-Sarnad, S. R. and Robinson, A.R. "BEF Analogy For Analysis of Box Girders", Proc. ASCE, Vol. 94, ST7, July 1968


TABLE 1 PLATE DIMENSIONS AND PROPERTIES

| Plate | Width (inches) | Thickness (inches) | Static Yield Stress[(a)] (ksi) | Ultimate Stress (ksi) | Elongation in 2 inches (%) |
|---|---|---|---|---|---|
| Top Flange | 7 (M1)<br>5-1/2 (M2) | 5/64 | 32.52 | 47.38 | 38.2 |
| Webs | 3 | 1/64 | 30.40 | 43.36 | 30.5 |
| Bottom Flange | 4-3/4 | 1/32 | 31.34 | 45.59 | 44.8 |

[(a)] Yield stress corresponding to zero strain rate

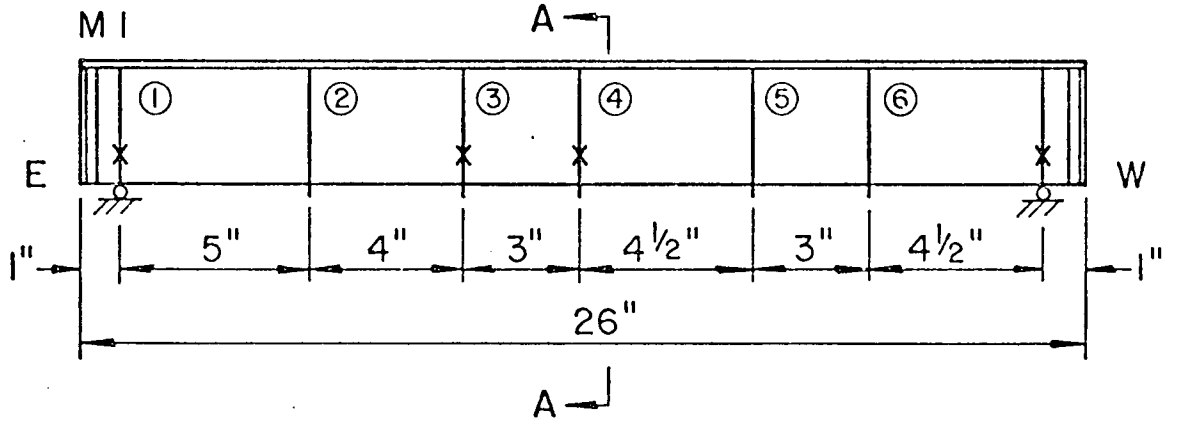


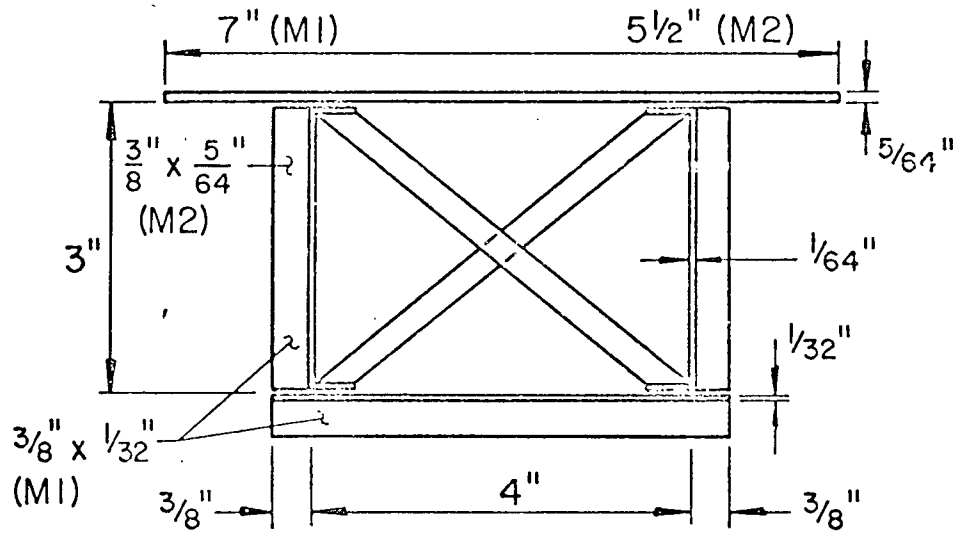


Section A - A

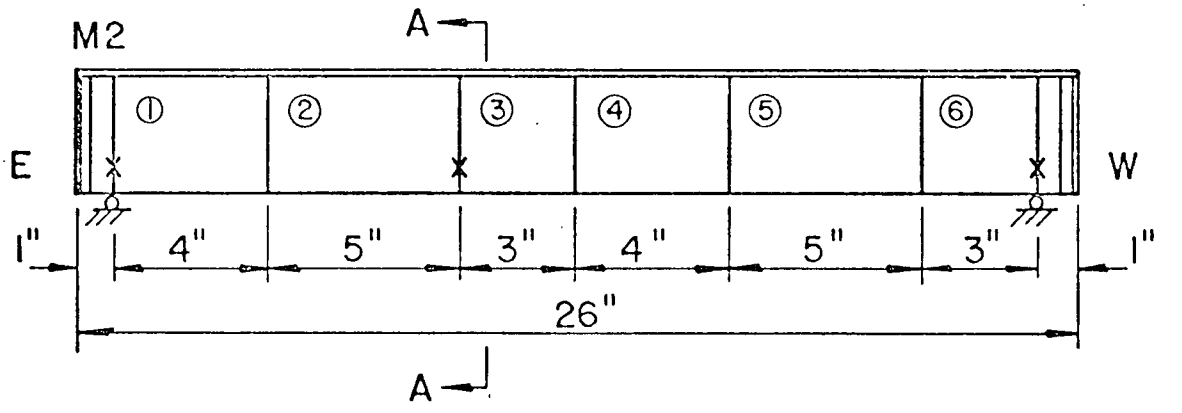


Fig. 1 Dimensions and Geometry of Specimens

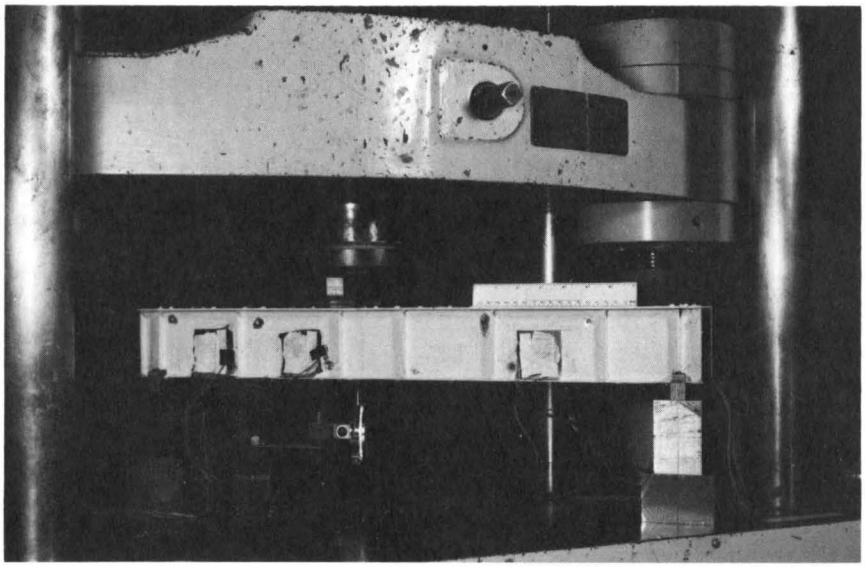

Fig. 2 Test Setup

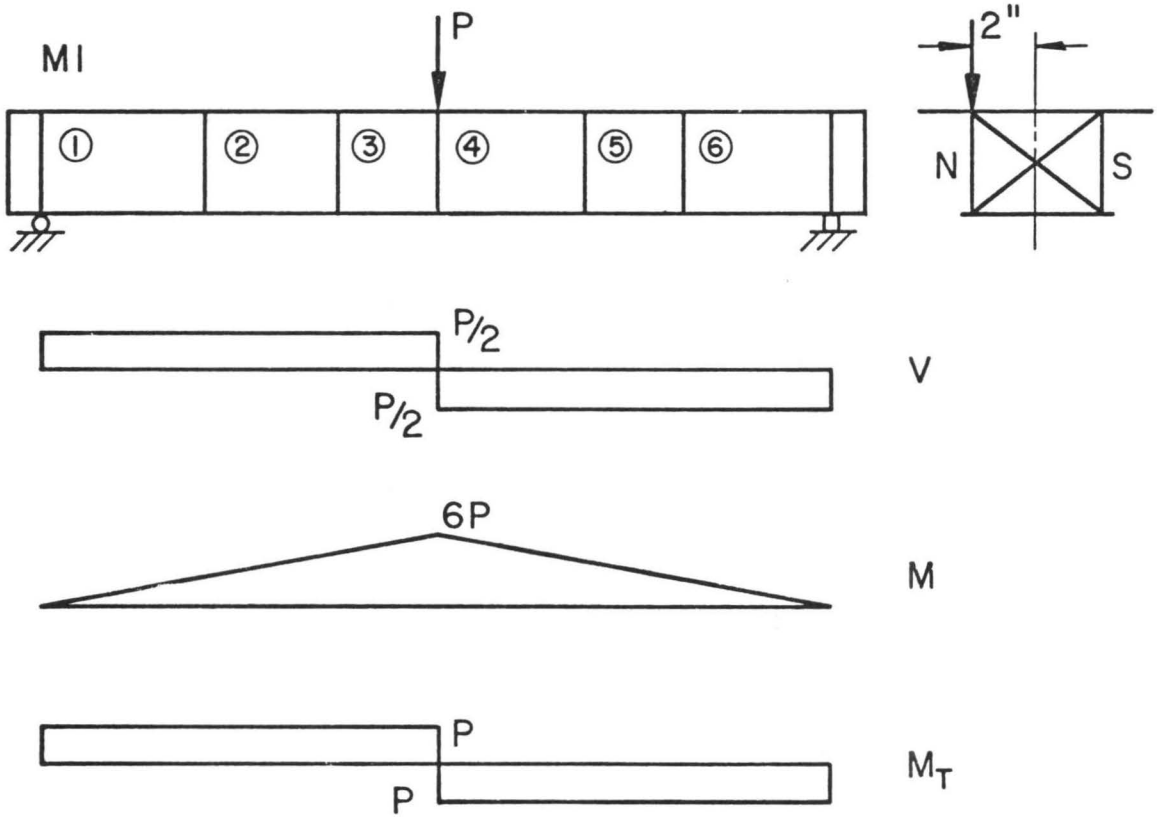


Fig. 3 Loading Conditions - Specimen M1

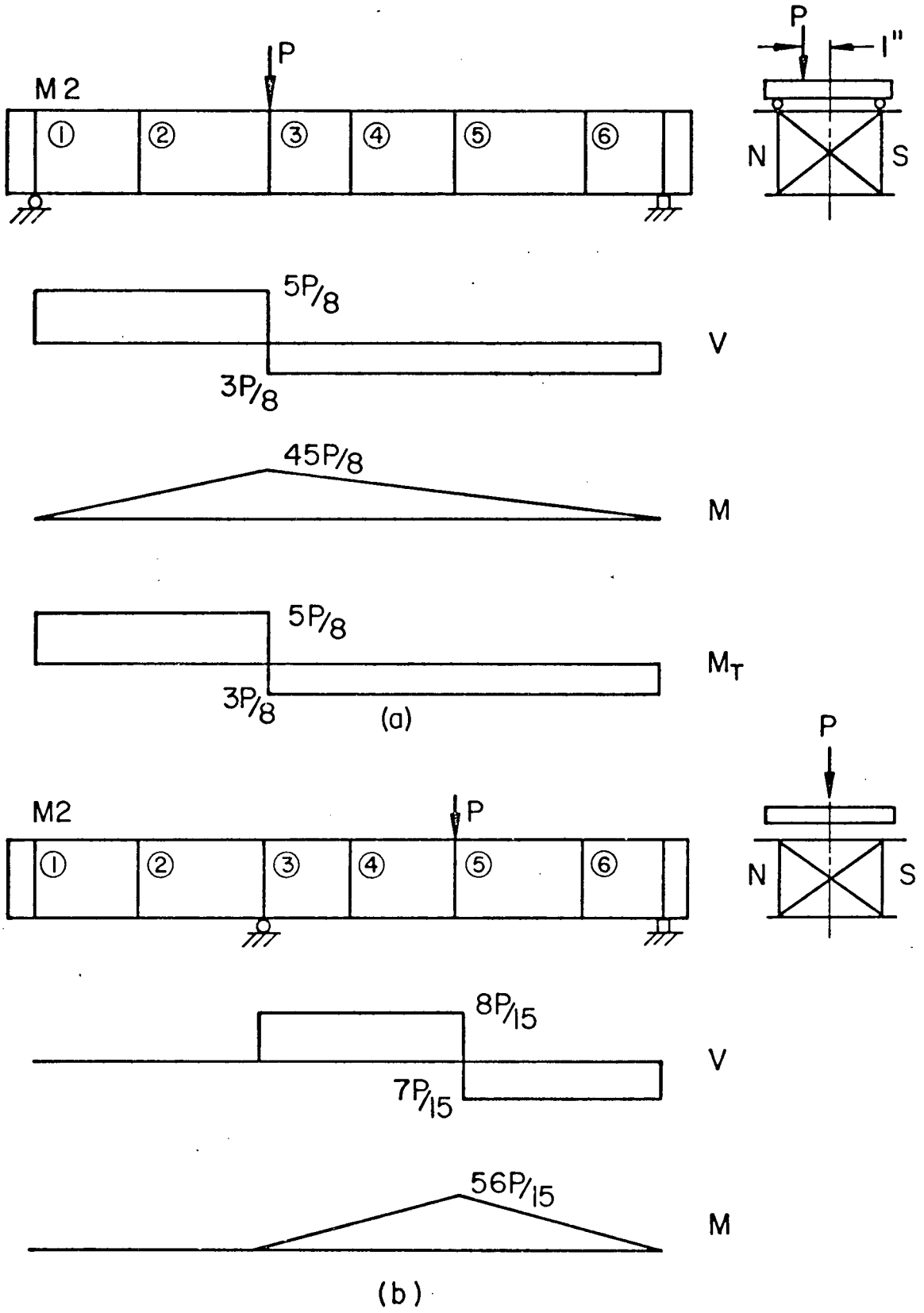


Fig. 4 Loading Conditions - Specimen M2

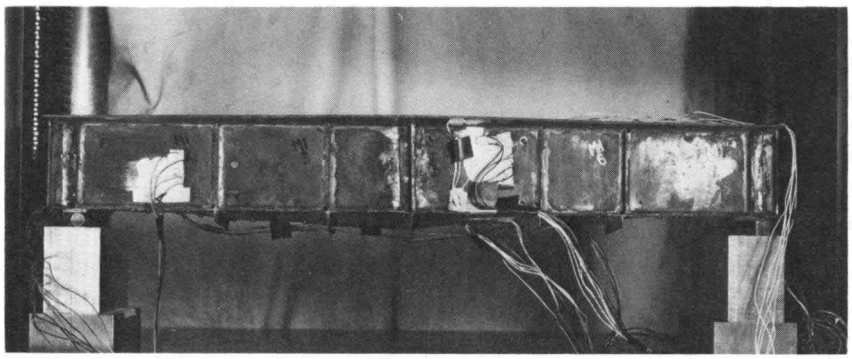

(a) North Side

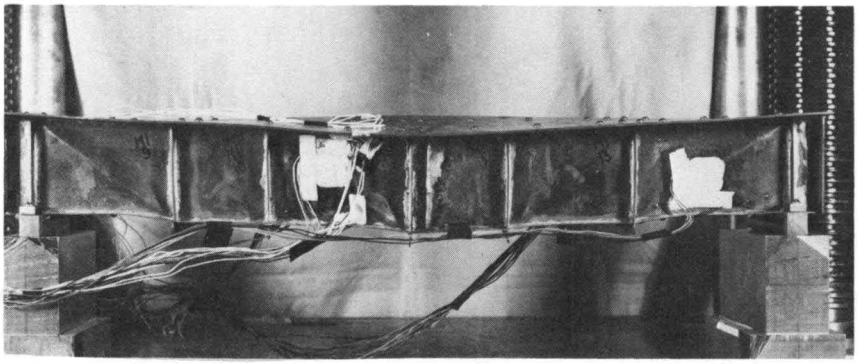

(b) South Side

Fig. 5 Overall Deformations - Specimen M1

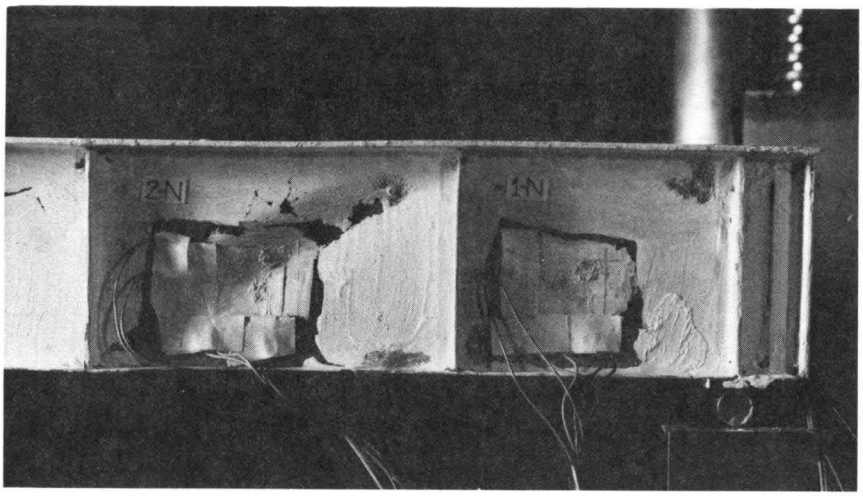


(a) Panels 1N and 2N

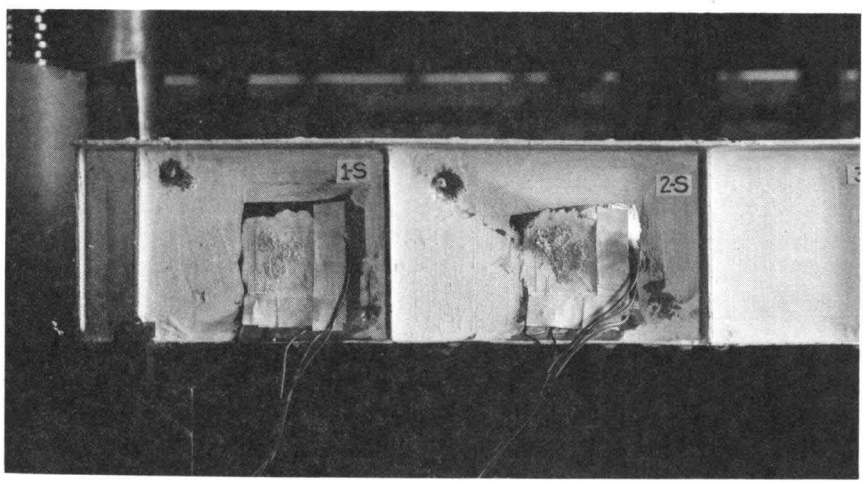


(b) Panels 1S and 2S

Fig. 6 Web Panel Deformations - Specimen M2
(Unsymmetrical Loading)

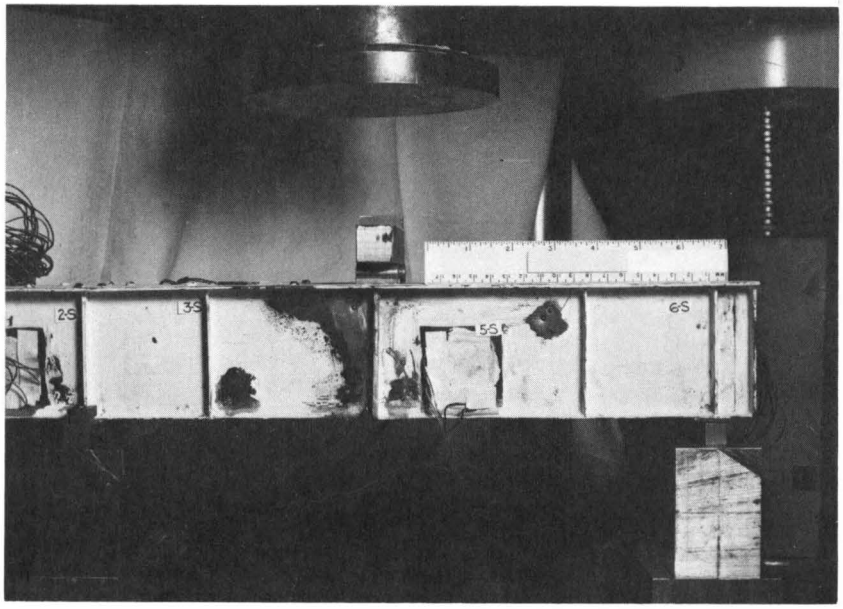


Fig. 7 Test Setup for Specimen M2
(Symmetrical Loading)

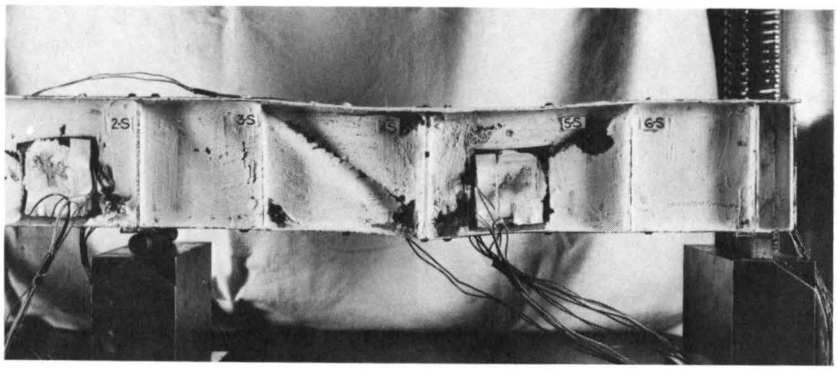


(a) South Side

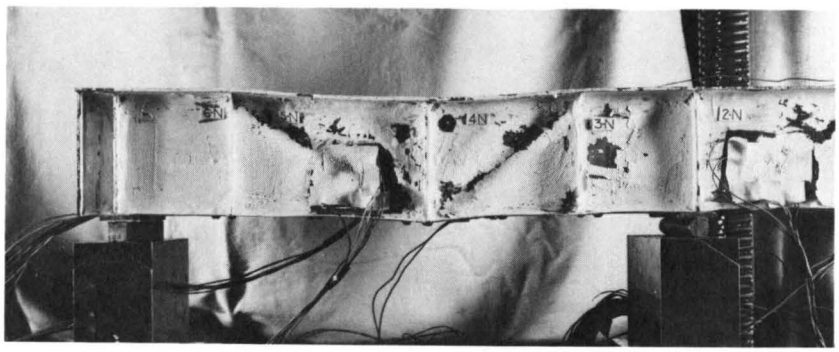


(b) North Side

Fig. 8 Overall Permanent Deformations - Specimen M2
(Symmetrical Loading)

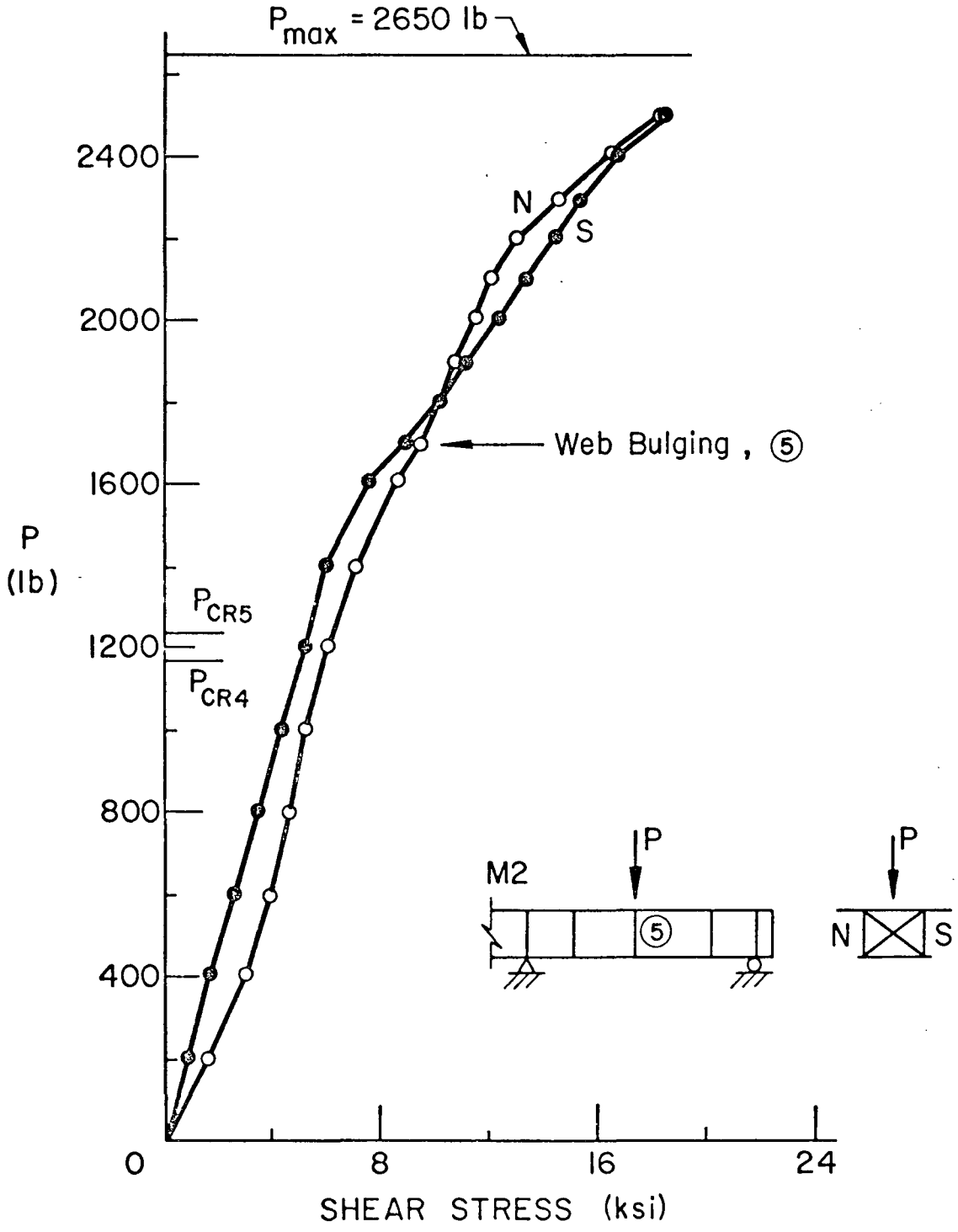


Fig. 9 Shear Stress at Centerline of Panel 5 - Specimen M2
(Symmetrical Load)

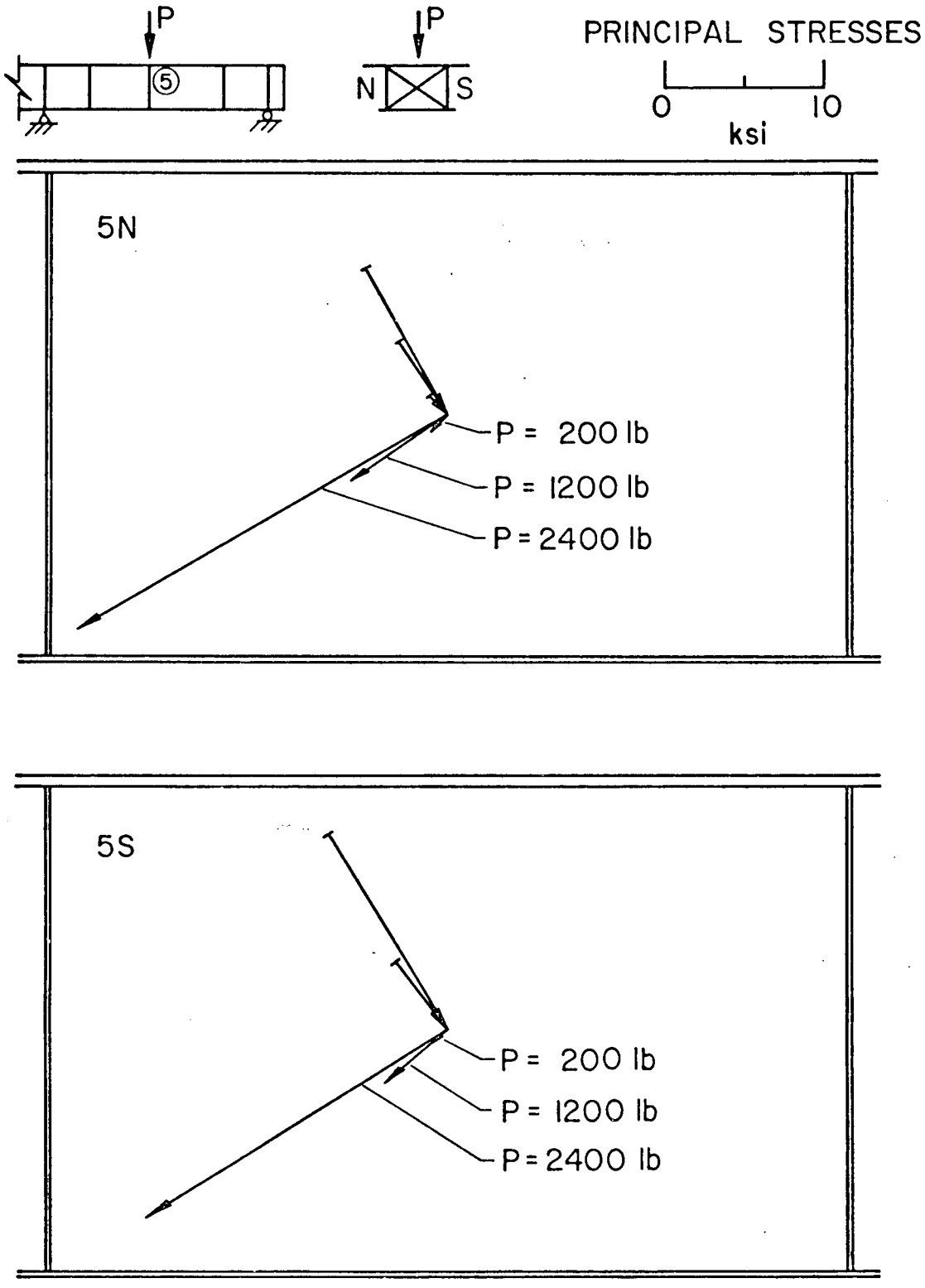


Fig. 10 Principal Stresses at Midpoint of Web Panels 5N and 5S - Specimen M2 (Symmetrical Load)

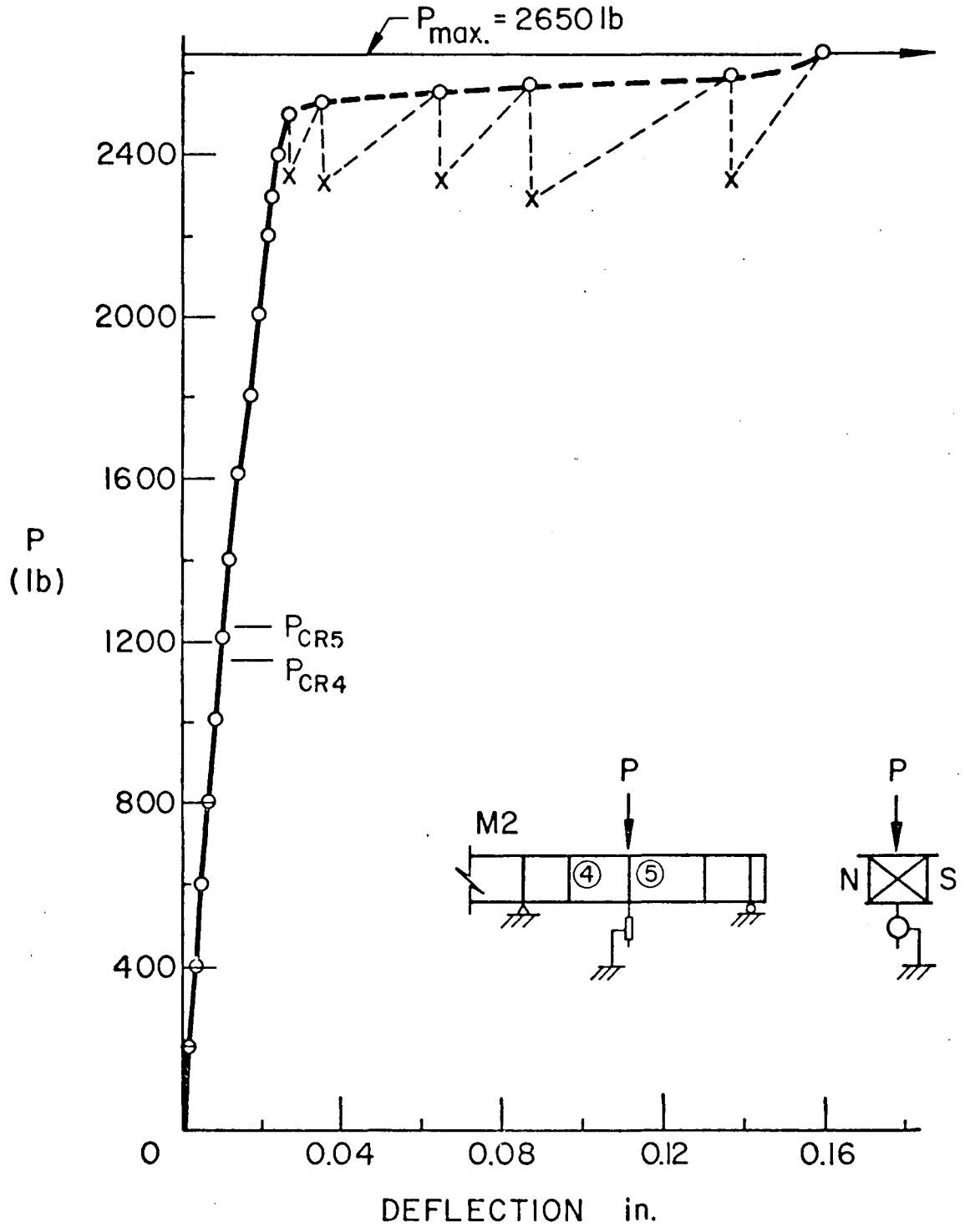


Fig. 11 Load-Point Deflection - Specimen M2
(Symmetrical Load)

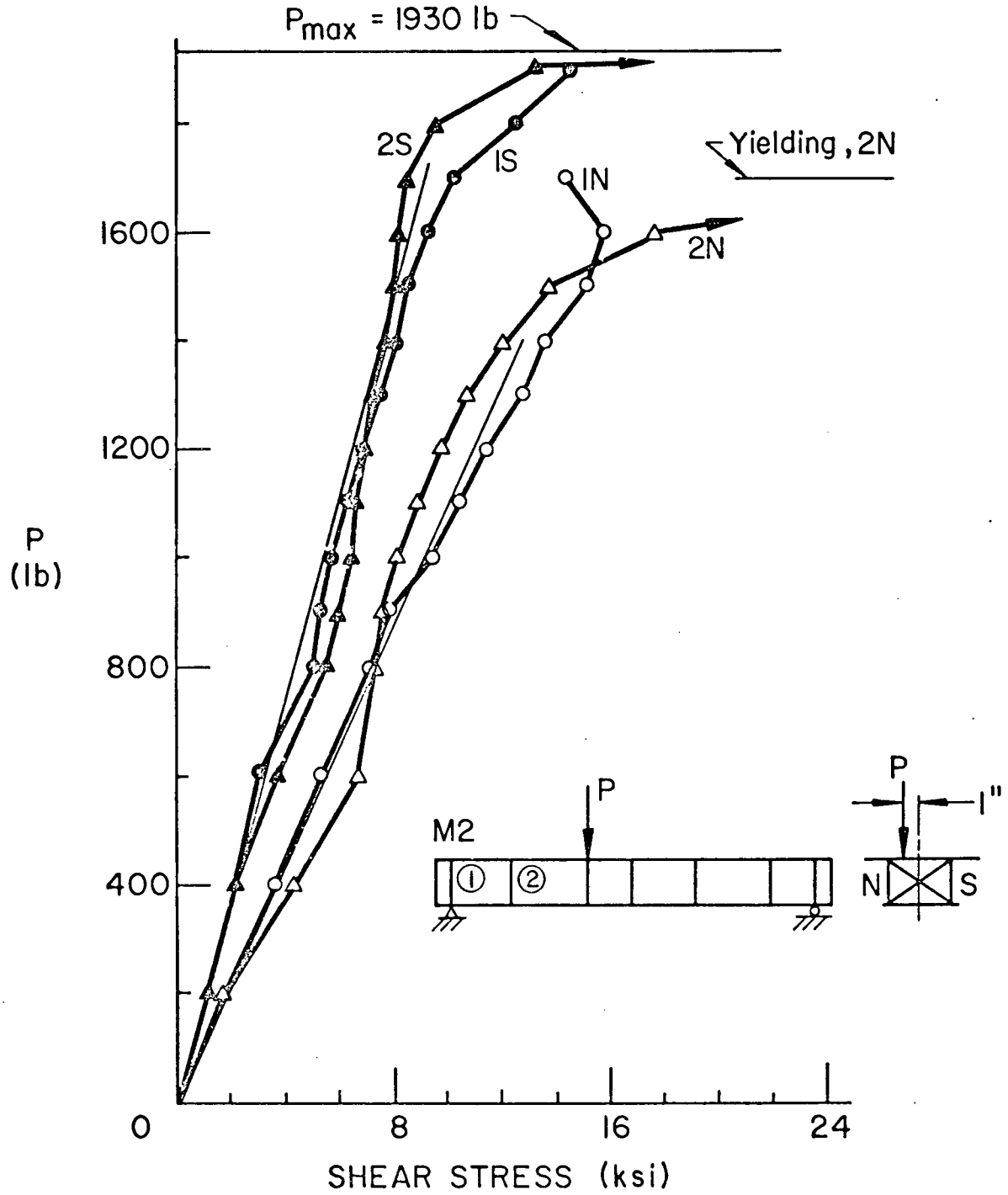


Fig. 12 Shear Stress at Centerline of Panels 1 and 2 - Specimen M2 (Unsymmetrical Load)

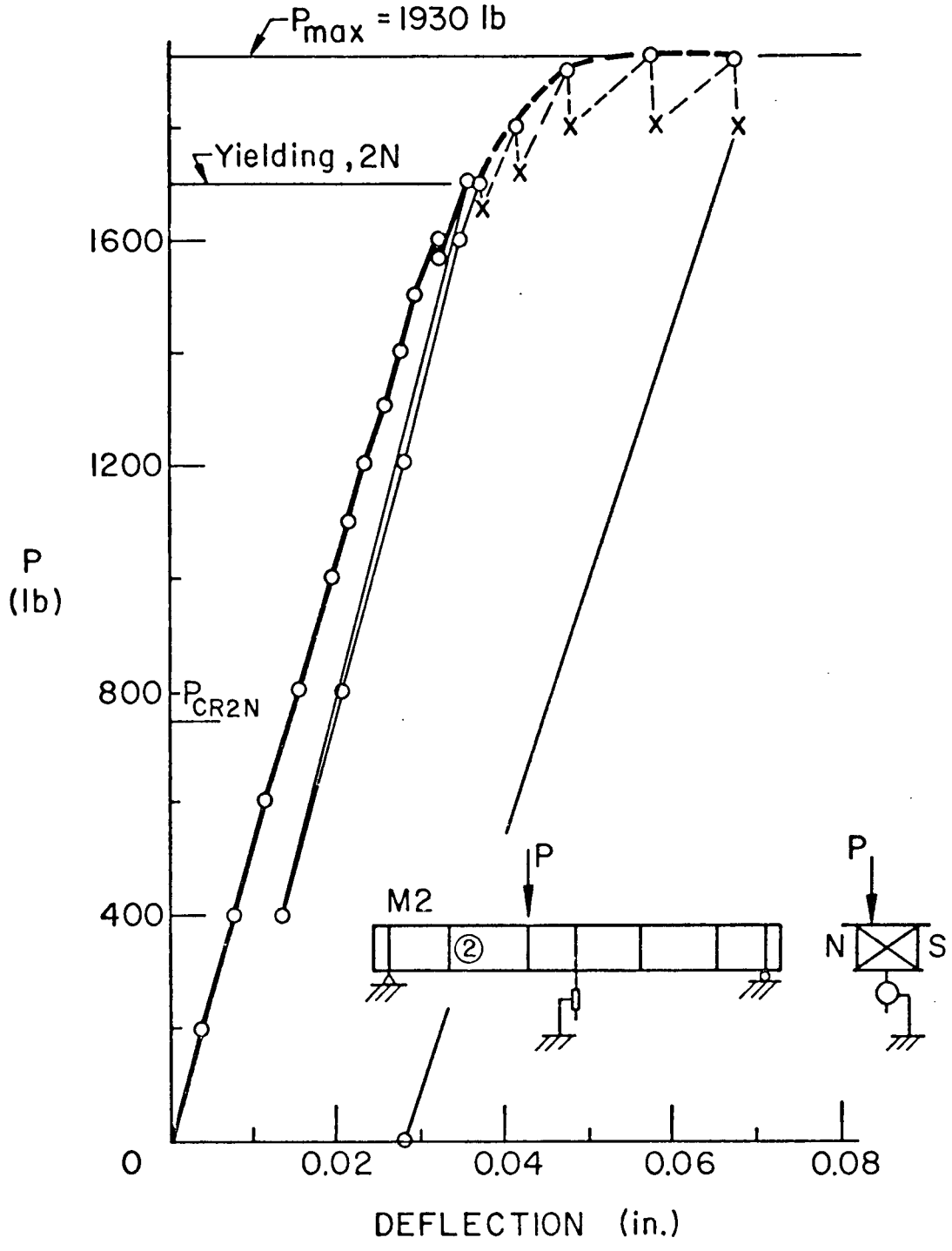


Fig. 13 Midspan Deflection - Specimen M2
(Unsymmetrical Load)

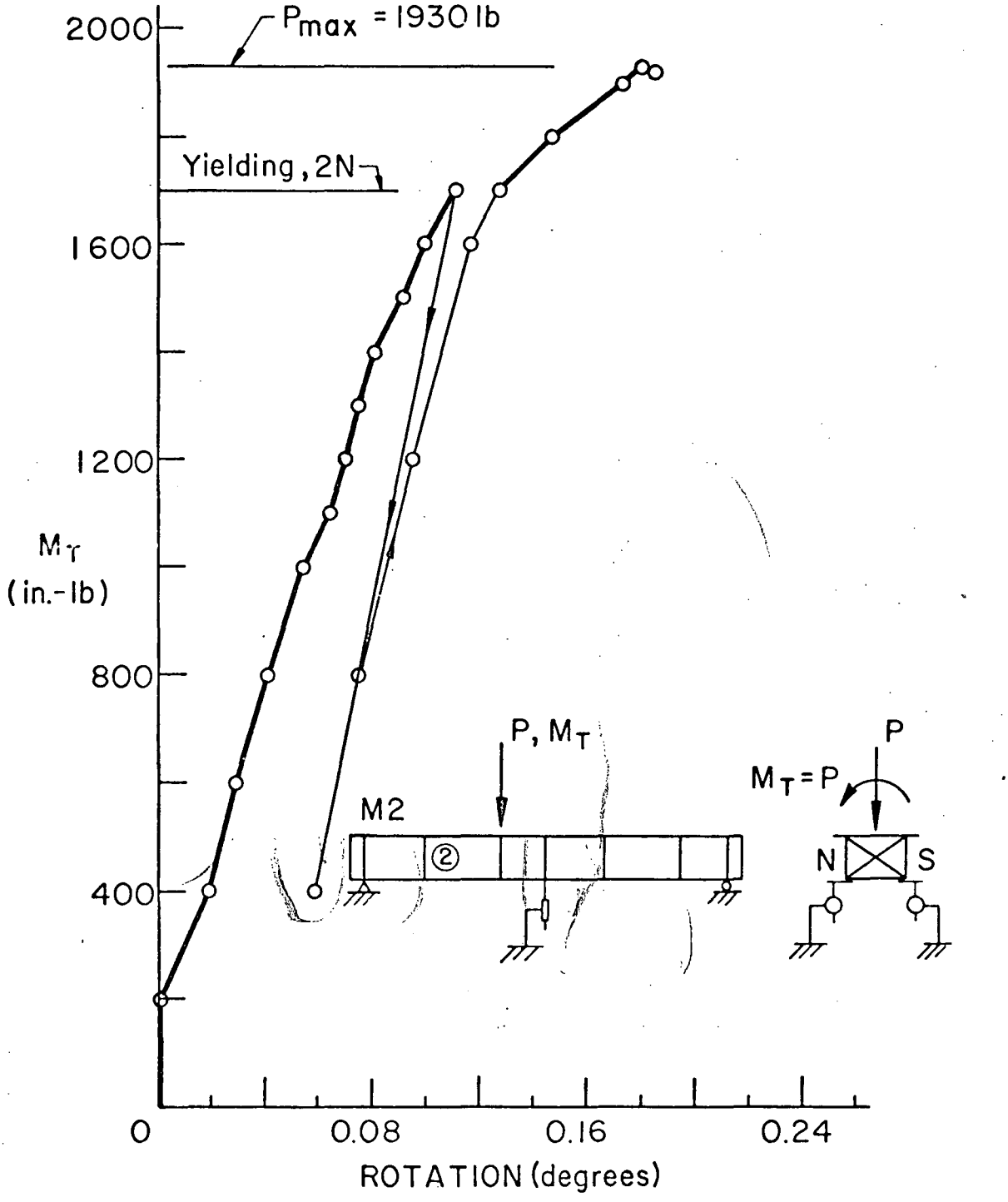


Fig. 14 Midspan Rotation - Specimen M2
(Unsymmetrical Load)

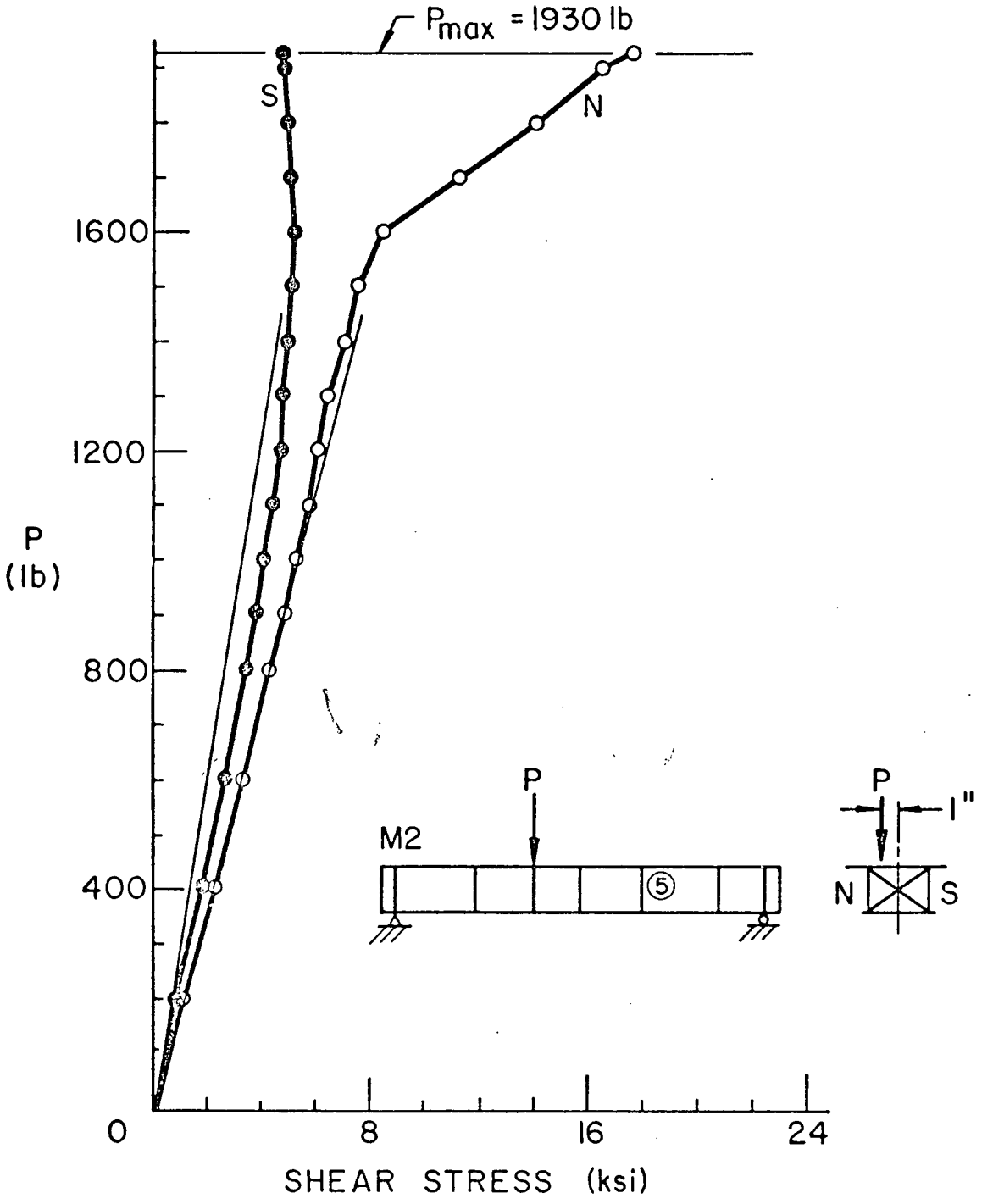


Fig. 15 Shear Stress at Centerline of Panel 5 - Specimen M2
(Unsymmetrical Load)

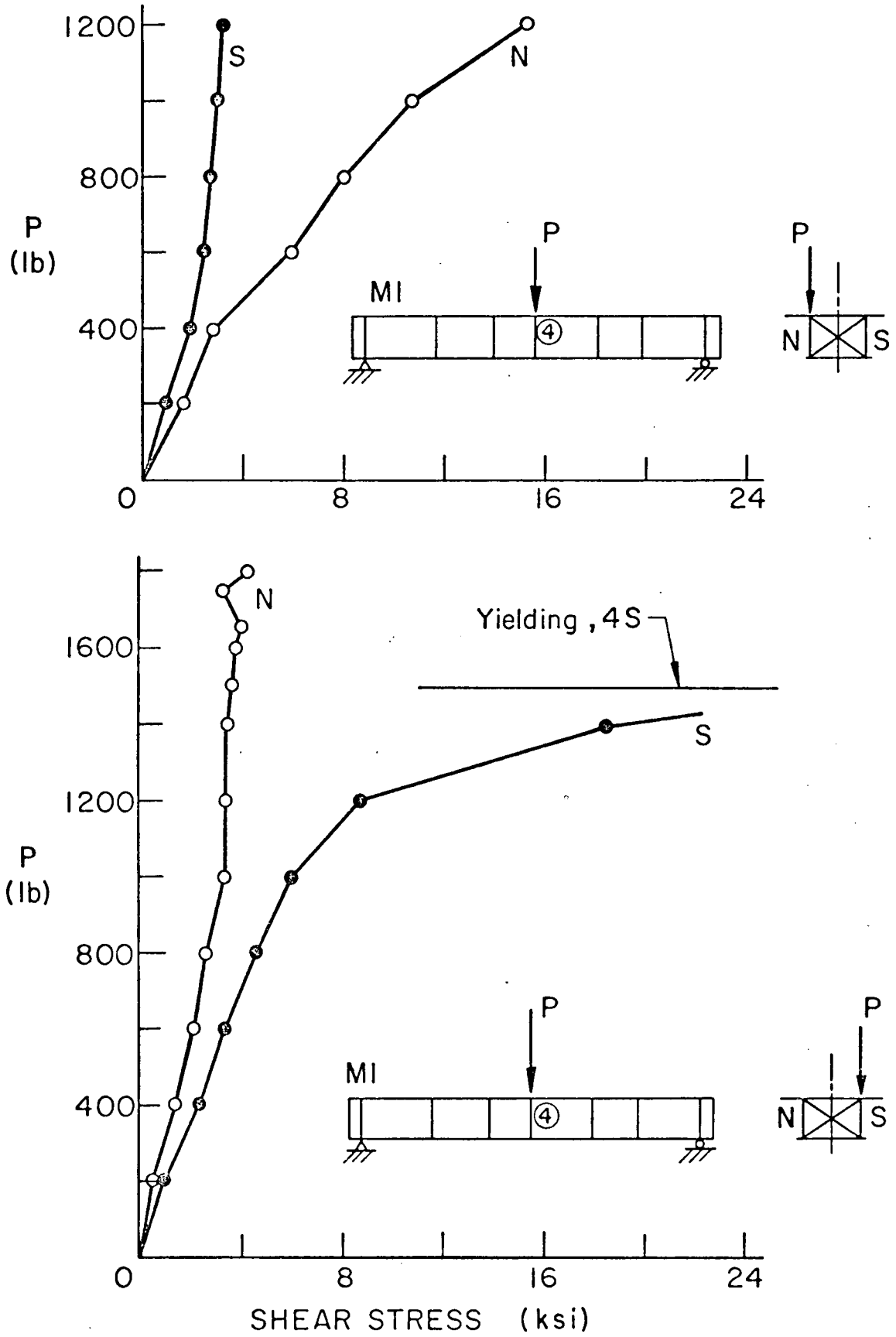


Fig. 16 Shear Stress at Centerline of Panel 4 - Specimen M1
(Unsymmetrical Load)

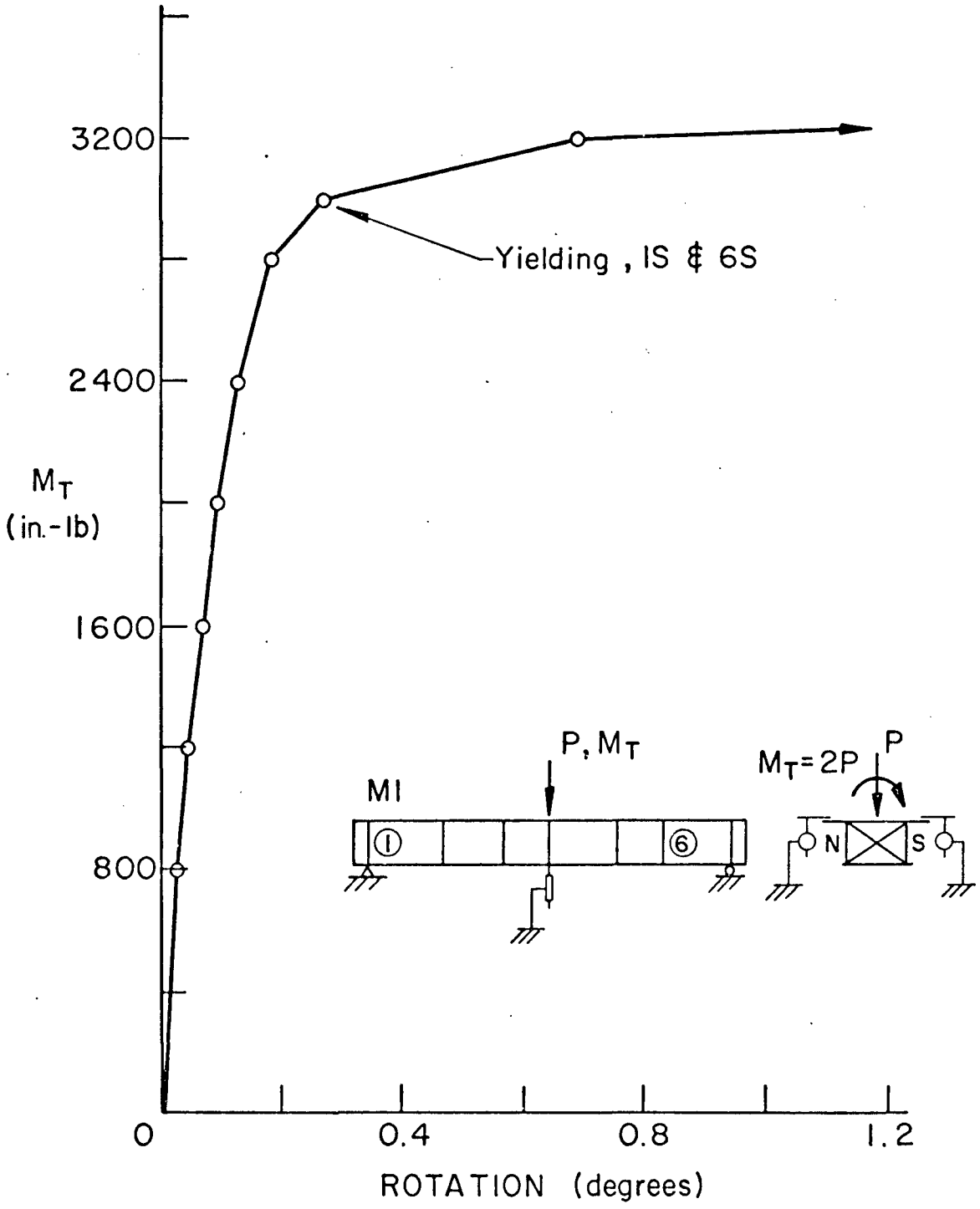


Fig. 17 Midspan Deflection - Specimen M1
(Unsymmetrical Load)

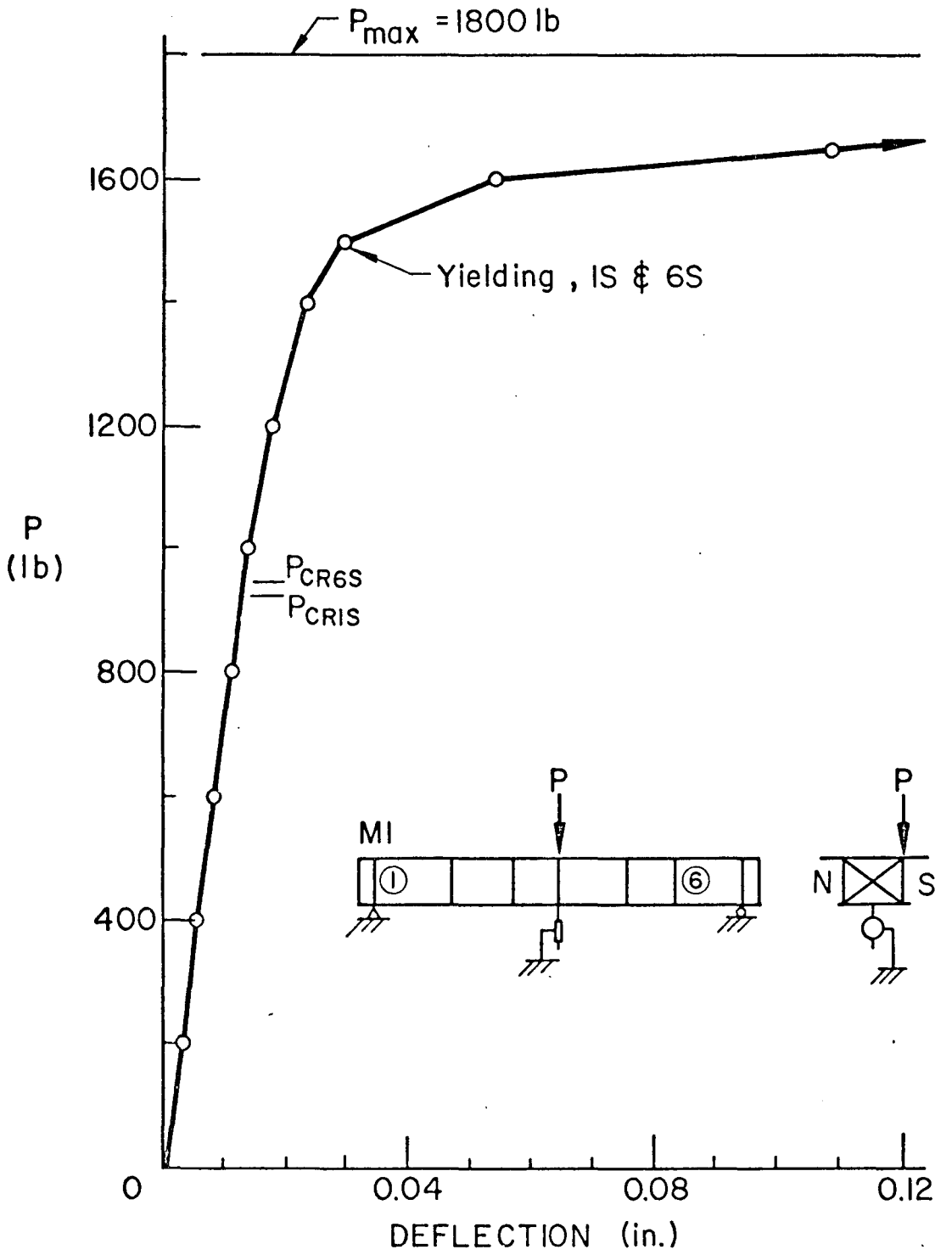


Fig. 18 Midspan Rotation - Specimen M1
(Unsymmetrical Load)